ISSN 0020-4412, Instruments and Experimental Techniques, 2014, Vol. 57, No. 5, pp. 572–578. © Pleiades Publishing, Ltd., 2014.
Original Russian Text © V.V. Kolobov, M.B. Barannik, V.N. Selivanov, D.V. Kuklin, 2014, published in Pribory i Tekhnika Eksperimenta, 2014, No. 5, pp. 61–67.

ELECTRONICS AND RADIO ENGINEERING

A Current Source with an Inductive Energy Storage for Measuring Pulse Impedances of Grounding Connections

V. V. Kolobov, M. B. Barannik, V. N. Selivanov, and D. V. Kuklin

Center for Physical and Technical Problems of Energy in the Northern Areas, Kola Science Centre, Russian Academy of Sciences (CPTPE NA, KSC, RAS), ul. Fersmana 14, Apatity, Murmansk oblast, 184209 Russia

e-mail: maxbar@ien.kolasc.net.ru

Received December 19, 2013

Abstract—A pulse generator with an inductive energy storage for measuring pulse impedances of grounding connections is developed. The generator produces current pulses with a rise time of 200–300 ns and an amplitude of up to 8 A. In contrast to the capacitive storage sources, it is fully controllable, allows one to adjust the amplitude, and ensures a constant current-pulse shape regardless of the load parameters. The different operation modes of the source are described. The experimental load-current waveforms are presented.

DOI: 10.1134/S0020441214040162

One of the factors affecting the reliability of protection of electrical installations and finally reliable operation of an energy system on the whole is the pulse impedance value of grounding connections (GCs) of substations and power transmission towers. The local pulse impedance of the GC is considered to mean the calculated value equal to the ratio of instantaneous pulse voltage at the grounding connection and the pulse current through it at times within the first units of microseconds, when the current flows only from the GCs coupled to the grounding mat of a substation and directly adjoining the studied grounded device [1].

Since under the pulse actions, there is no such commonly accepted characteristic of the GCs as, e.g., the concept of stationary resistance R at low-frequency actions [2], to determine pulse characteristics of the GCs, it is necessary to have curves of the GC current and voltage, which can be further processed using different algorithms. Examples of these experimental curves of currents and voltages at the GCs and the calculated instantaneous resistance of the GC are given in [2].

The experimental procedure for determining the pulse characteristics of the GCs is based on measurements of resistances by the three-electrode method [1, 3, 4]. The experimental setup contains a pulse current generator, two lengthy conductors, which form the current and potential lines with a characteristic impedance of about 400 Ω in pulse measurements, primary current and voltage sensors, and a digital two-channel oscilloscope. As conductors, the sheath of 100-m length coaxial cables is used.

The generator forms in the current line pulses with necessary amplitude and time characteristics. The initial data for calculating the impulse grounding resistance is the current and voltage pulse waveforms recorded by the digital oscilloscope in the corresponding lines.

As a generator, a pulse current source, based on a capacitive storage, is used in these studies. In this source, the current pulse is formed, when a spark gap operates with the subsequent discharge of the storage capacitor into the load. The experience of applications of these generators showed that the current and voltage pulse shapes can be strongly distorted due to a nonuniform distribution of the characteristic impedance along the current line and reflections from its end.

In addition, in conditions of soils with a high resistivity, long transient processes arise at the start of voltage pulses (the leading edges of recorded voltage pulses lengthen). These distortions of the shape of analyzed pulses complicate the reliable determination of the pulse grounding resistance.

To avoid this situation, it is necessary to ensure a constant pulse shape in the current line regardless of the degree of its matching and distribution of the characteristic impedance along it. A constant current-pulse shape can be ensured, if the current source with an inductive energy storage is used as a generator.

We designed a current source with an inductive energy storage for measuring pulse resistances of the GCs. Since the magnetic-field energy storage in the inductance coil and the current in the choke cannot change stepwise [5], the pulse current generator, which is based on an inductive storage, is capable of holding a constant pulse-current amplitude in the line with changing load parameters in a time interval sufficient for performing measurements.

The main elements of this current-pulse generator are an inductive energy storage and an opening switch. As an inductive storage, transformer *Tr* acts, and transistor *Q* acts as a disconnecting switch (Figs. 1a, 1b). The generator is based on the flyback converter scheme [6], in which the energy storage phase and the phase of its transmission to the load are time-independent, and the step-up transformer is actually a two-winding storage choke [7]. In the energy storage phase, the inductive storage transistor *Q* is enabled (Fig. 1a). Current I_L in the inductance of the primary winding of the transformer will go up until the enabling voltage U_{en} is available at the transistor gate. The current rise rate can be written as

$$\frac{dI_L}{dt} = \frac{U_C}{L_\mu}, \tag{1}$$

where L_μ is the magnetizing inductance of the transformer and U_C is the voltage across the supply capacitor of the stage. By the completion moment of the energy storage phase (t_{st_e} in the current and voltage timing diagrams shown in Fig. 1c), the current in the primary winding reaches the maximal value:

$$I_{L\max} = \frac{U_C \Delta t}{L_\mu}. \tag{2}$$

When switch *Q* is disabled, the energy transmission phase to the load starts (Fig. 1b). Due to the self-induction, the polarity of voltage U_L of the primary winding of the transformer *Tr* changes to the opposite one, the diode *D* is enabled, and the energy stored in the choke goes into the load.

In the current line connected to the generator output, a current pulse is formed (Fig. 1c), for which it can be written $I_{ld} = I'_{ld}/k_{tr}$, where k_{tr} is the transformation ratio ($k_{tr} > 1$), and I'_{ld} is the load current reduced to the primary winding and described by the expression:

$$I'_{ld} = I_{L\max} e^{-\frac{t}{\tau}}. \tag{3}$$

The time constant τ is determined as:

$$\tau = \frac{L_\mu}{Z'_{ld}}, \tag{4}$$

where Z'_{ld} is the load impedance reduced to the primary winding.

In this case, the surge voltage U_L arises at the primary winding of the transformer. This voltage much exceeds the supply voltage U_C of transistor *Q* and can be written as

$$U_L = \frac{U_{ld}}{k_{tr}} = \frac{I_{ld} Z_{ld}}{k_{tr}}. \tag{5}$$

The voltage at terminals of the switch element *Q* is

$$U_{sw} = U_C + U_L = U_C + \frac{I_{ld} Z_{ld}}{k_{tr}}. \tag{6}$$

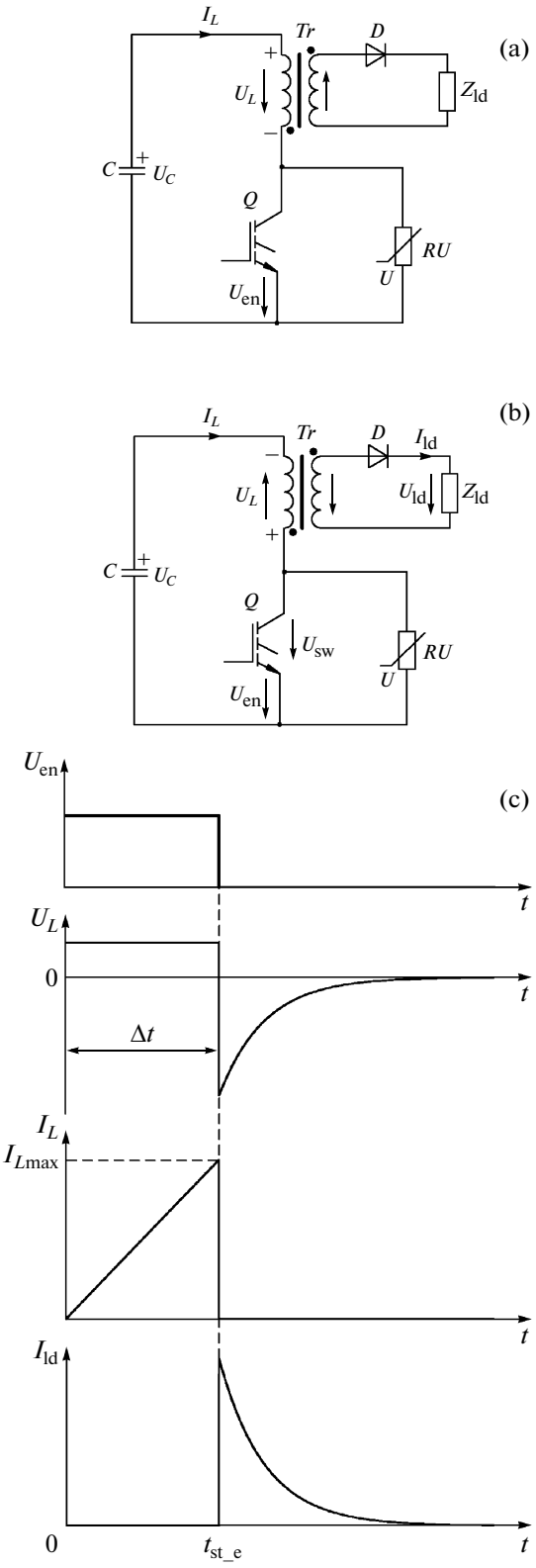

Fig. 1. Phases of operation of the inductive storage: of (a) charge; (b) discharge; and (c) timing diagrams of currents and voltages.

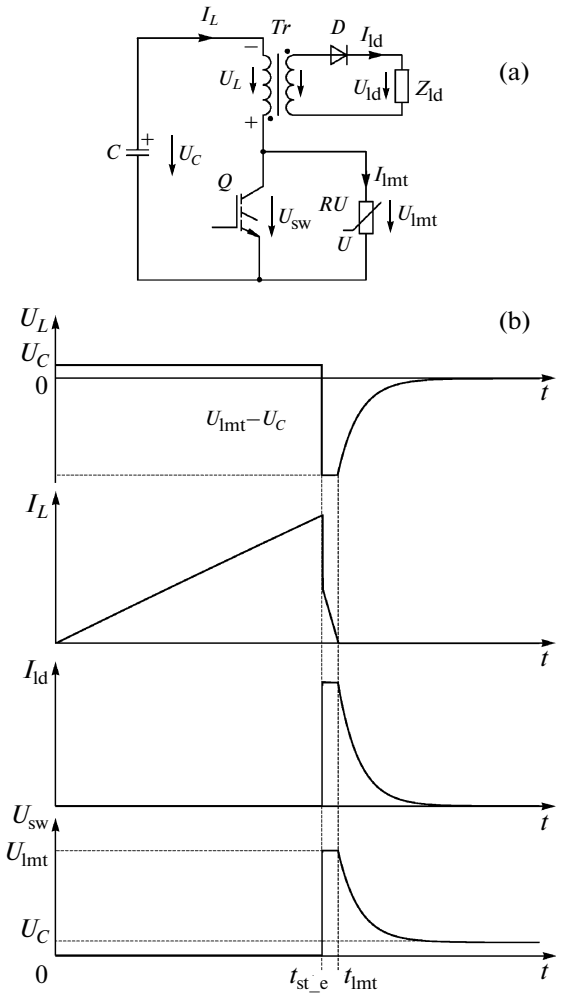

Fig. 2. (a) Circuit of the output stage of the current source with an inductive storage and (b) timing diagrams explaining the source operation at $Z_{ld}I_{ld} > U_{ad}$.

For time moment t_{st_e} ($t = 0$ for expression (3)) one can write as:

$$U_{sw} = U_C\left(1 + \frac{Z_{ld}dt}{L_\mu k_{tr}^2}\right). \quad (7)$$

Thus, for the fixed voltage U_C, known charging time dt, and specified design parameters of the inductive storage, which determine k_{tr} and L_μ, the voltage at the transistor directly depends on the load impedance Z_{ld} of the generator.

The peculiarity of operation of the described current source is the presence of wave processes in its load (current line). The load impedance Z_{ld} of the generator is formed from the resistance of the studied GC and the line resistance, which is determined by pulse processes within the first microsecond (current-wave travel time to the line end and back). Depending on the degree of matching of the grounded line end, upon the completion of the double travel time, this component can be determined by a relatively small characteristic impedance of the line or tend to the grounding resistance of its end, which can be significant.

Thus, even provided that transistor Q is correctly selected with respect to the admissible working voltage class, with significant value Z_{ld}, voltage U_{sw} may exceed the maximal admissible collector–emitter voltage $U_{ce\ max}$, thus leading to the breakdown of switch Q. The break of the conductor of the current line is also possible ($Z_{ld} = \infty$). To protect the transistor against a potential breakdown, a varistor (RU in Fig. 2a) with limitation voltage U_{lmt} below $U_{ce\ max}$ is connected in parallel to it.

Let us introduce the concept of the admissible output voltage U_{ad}, i.e., the maximal voltage at the generator output, at which the varistor does not yet limit the voltage across the switch. Let us consider the operation of the output stage of the current source with an inductive storage, when the output voltage exceeds the U_{ad} value, if the condition $Z_{ld}I_{ld} > U_{ad}$ is fulfilled. For the admissible voltage, one can write as follows:

$$U_{ad} = k_{tr}(U_{lmt} - U_C) \quad (8)$$

or in the values reduced to the primary winding:

$$I'_{ld} = \frac{U_{lmt} - U_C}{Z'_{ld}}. \quad (9)$$

The current through varistor RU in the conducting state is

$$I_{lmt} = I_L - I'_{ld}. \quad (10)$$

The scheme in Fig. 1a is true in the charging phase of the inductive storage (interval from 0 to t_{st_e} in Fig. 2b), and the current in the inductive storage is determined by expression (1). For the energy transmission phase to the load in interval t_{st_e}–t_{lmt}, when varistor RU is in the conducting state, it can be written:

$$\frac{dI_L}{dt} = \frac{-(U_{lmt} - U_C)}{L_\mu}. \quad (11)$$

After decreasing the output voltage to U_{ad} (after time moment t_{lmt}), the shape of the load current, reduced to the primary winding of the transformer, is described by the expression:

$$I'_{ld} = \frac{U_{lmt} - U_C}{Z'_{ld}} e^{-\frac{t}{\tau}}. \quad (12)$$

Note that for a high-resistance load of the current source, to prevent the operation of varistor RU according to (7), it is possible to decrease the charging-phase duration of the inductive storage dt and thus ensure the fulfillment of the relationship $Z_{ld}I_{ld} < U_{ad}$.

Upon the completion of the double travel time of the current wave along the line $2T_{trav}$, which is approximately equal to 0.9 μs, the generator load can be considered a parallel circuit (loop) with lumped parameters. The loop includes the capacitance of the cable of the current line to the earth C_{ld}, impedance Z_{ld}, basi-

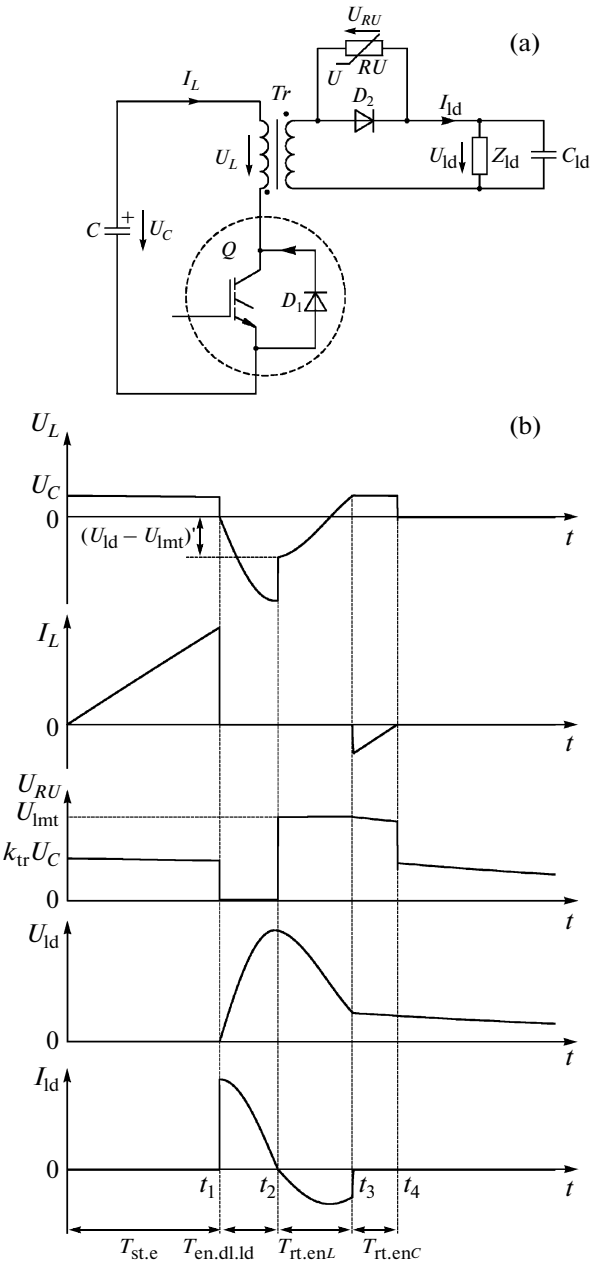

Fig. 3. (a) Circuit of the output stage of the current source with an inductive storage and (b) timing diagrams explaining the source operation with the periodic current in the load.

cally determined by the grounding quality of the line end, and the magnetizing inductance of the inductive storage transformer L_μ.

Depending on the ratio of impedance Z_{ld} and characteristic (wave) impedance of the loop, the current in the load may be both aperiodic and periodic. The latter arises, if the following condition is fulfilled:

$$Z_{ld} < \frac{1}{2}\sqrt{\frac{L_\mu}{C_{ld}}}. \quad (13)$$

The circuit of the output stage of the current source and timing diagrams that clarify the generator operation in this mode are shown in Fig. 3. The generator cycle that produces a current pulse in the load can be divided into four phases:

1. Energy-storage phase of the inductive storage (T_{st_e} in Fig. 3b). The charging process of the inductive storage is already described above. In the charging phase, the reverse voltage equal to $k_{tr}U_C$ is applied to diode D_2 (Fig. 3a).

2. The inductive-storage discharge and energy delivery to the load ($T_{en.dl.ld}$ in Fig. 3b). In this phase diode D_2 is open, and the current in the load is capacitive and decreases within time $T_{en.dl.ld}$ down to zero, and the voltage across the load goes up. At time moment t_2, the current reverses direction and, in this case, the voltage arises at the closed diode D_2 , which can significantly exceed the maximal admissible constant reverse voltage of the diode $U_{rev\,max}$. The parallel varistor (RU in Fig. 3a) is intended to prevent the diode breakdown. Its limitation voltage U_{lmt} is selected so that $U_{lmt} < U_{lmt\,max}$.

3. At time moment t_2, the phase of energy return from the load to the inductive storage starts ($T_{rt.enL}$ in Fig. 3b). The energy stored in the load capacitor is converted into the energy of the magnetic field of transformer Tr. The inductive storage is in a way charged from the secondary winding. During this process, the voltage across the primary winding of the inductive storage $(U_{ld} - U_{lmt})'$ decreases to zero and, then, having changed the sign, starts increasing until it becomes equal to the stage supply voltage U_C.

4. After the condition $(U_{ld} - U_{lmt})' \le -U_C$ is established, the antiparallel diode D_1 of switch Q is enabled at time moment t_3 (Fig. 3b), and the energy stored in the choke is transmitted to the power-supply capacitor C (current pulse I_L in the graph). The phase of the energy return to the capacitor, designated in Fig. 3b as $T_{rt.enC}$ is over at time moment t_4. Further, the residual voltage U_{ld} of the load slowly declines to zero owing to the discharge of capacitor C_{ld} through impedance Z_{ld}.

A schematic diagram of the current source, based on the inductive energy storage, is shown in Fig. 4. The basic elements of the inductive storage are the transformer Tr and IGBT transistor Q_3. The transformer design uses two E-shaped 00K5528E026 cores (Magnetics Co.) [8] (the length of the centerline is 12.3 cm, the cross-section is 3.5 cm^2, and the volume of the magnetic circuit is 43.1 cm^3), based on Kool Mμ's material. The Kool Mμ cores are made of an alloy of iron and aluminum [9] and characterized by a high saturation induction B_M, small losses at high frequencies, and a low permeability μ, thus allowing one to

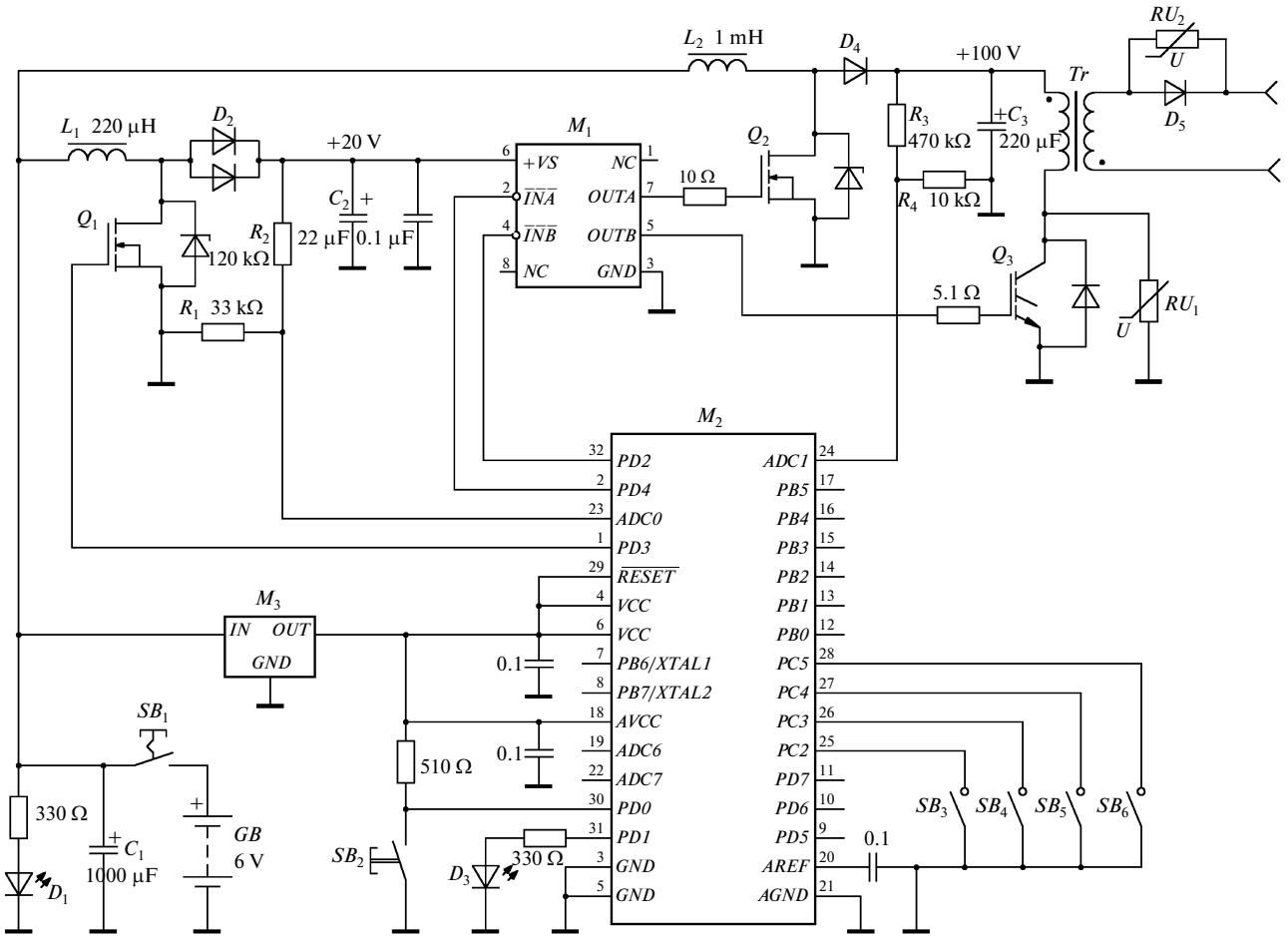

Fig. 4. Schematic diagram of the current source for measuring pulse resistances of the grounding connections based on the inductive energy storage: (M_1) IR4426S; (M_2) ATmega48PA; (M_3) 78L05; (Q_1) IRLML0030TR; (Q_2) IRF640; (Q_3) IRG7PH35UD1; (D_1) BL-L513LRC; (D_2) BAV70; (D_3) BL-L532UWC; (D_4) UF4007; (D_5) HER207; (RU_1) TVR20681; and (RU_2) S10K420.

increase the Q-factor of the inductive storage. For the used core, $\mu = 26$ and $B_M = 1.05$ T.

The primary winding is made of 0.57-mm ПЭВ2 double wire and contains 48 turns; the secondary winding contains 383 0.3-mm ПЭВ2 wire turns. To decrease the leakage inductance L_S leading to stretching of the leading edges of produced current pulses, the windings are sectionalized. Simultaneously, gaps are provided between the windings to decrease the interwinding capacitance of the transformer, which results in the onset of parasitic oscillations on the current-pulse plateau.

As Q_3, an IRG7PH35UD1 International Rectifier IGBT transistor ($V_{CES} = 1200$ V, $I_{NOM} = 20$ A) [10] is used. It features a small switching time, low dynamic losses and conduction losses, and a rectangular reverse biased safe operating area (RBSOA). The latter is especially important in the described circuit, where transistor Q_3 that breaks the current through the inductive storage operates at the RBSOA boundary. The function of the both varistors (RU_1 and RU_2) is described above. One of the channels of microcircuit M_1 (control driver of the IGBT and MOSFET switches) is used to control the gate of Q_3.

The considered pulse current source for measuring the pulse impedances of the GCs is the portable small-size unit and has a self-contained power source. As this source, a lead-gel chargeable cell *GB* with a voltage of 6 V is used. To form the necessary (100 V) voltage for charging the inductive storage, a stabilized pulse step-up voltage converter, containing elements L_2, Q_2, D_4, and C_3, is used.

The second channel of driver M_1 is used to control the gate of Q_2. The supply voltage of microcircuit M_1 determines its output voltage and is 20 V in the considered circuit. This control voltage of the gate of transistor Q_3 is required for ensuring the rectangular RBSOA [10].

The second step-up converter, forming the supply voltage of microcircuit M_1, is based on elements L_1,

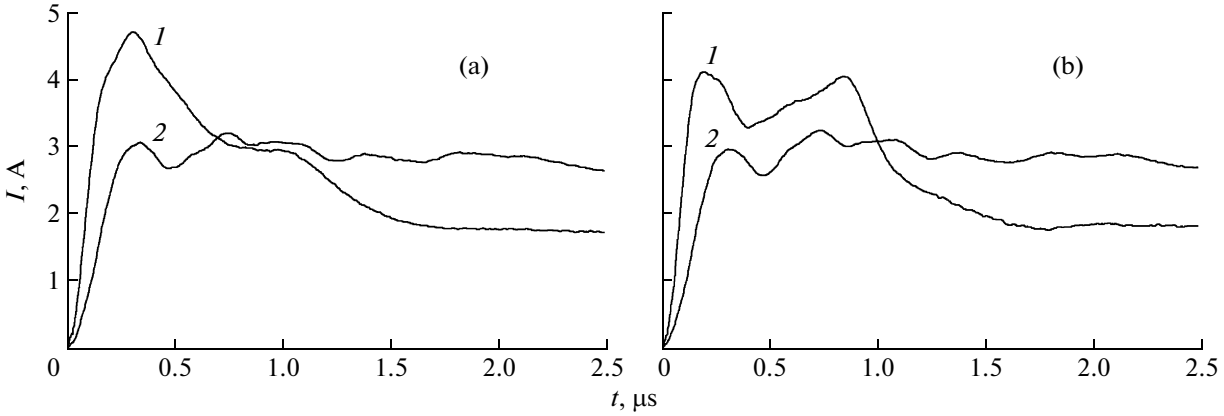

Fig. 5. Experimental oscillograms of the current pulses through the grounding connection with the generator based on (*1*) capacitive and (*2*) inductive storages: (a) with a nonuniform distribution of the characteristic impedance along the current line, and (b) with reflection from the line end.

Q_1, D_2, and C_2. Transistor Q_1 is controlled by the logic level. Therefore, its gate is directly connected to the digital output *PD3* of microcontroller M_2.

An 8-bit ATmega48PA AVR microcontroller is applied for producing the control signal of the disabling switch of the inductive storage [11]. By regulating the charging phase duration of the inductive storage, it is possible to change the stored energy and, hence, amplitude of the output current pulse.

In the described generator this regulation is carried out by switches SB_3–SB_6, which produce a 4-bit binary code. The current-pulse formation is triggered by button SB_2. It is also possible to use an external trigger from the signal applied at one of digital inputs of the microcontroller.

At the same time, microcircuit M_2 acts as pulse-width-modulation controllers for step-up stabilized voltage converters. A feedback signal from converter outputs (capacitances C_2 and C_3 in Fig. 4) after voltages dividers (R_1, R_2 and R_3, R_4) arrives at inputs *ADC0* and *ADC1* of the built-in ADCs of microcontroller M_2. The microcontroller is powered from a linear stabilizer on microcircuit M_3.

The generator forms current pulses with a rise time of 200–300 ns and an amplitude of up to 8 A in the load.

The experimental oscillograms of the current pulses through the GC, which were recorded with the help of a generator based on capacitive (curves *1*) and inductive (curves *2*) storages, are shown in Fig. 5 for comparison. The inflection of the current curve (*1* in Fig. 5a) near 0.3 μs is caused by a significant change in the characteristic impedance in the corresponding part of the current line.

In the current curve *1* (Fig. 5b), the sharp inflection is observed at a time of 0.9 μs. It is caused by the reflection of the current wave due to the absence of matching at the line end. In both cases, the shape of curve *2* of the current pulse, which is formed by the inductive storage-based generator, is preserved.

It is necessary to note that, in addition to providing the constant pulse shape in the current line and the possibility of regulating its amplitude, the current source based on the inductive energy storage possesses another advantage, as compared to the capacitance-storage source, namely, it is controllable. In the pulse-current generator based on a capacitance storage, the output current pulse is formed, as a rule, by an uncontrolled high-voltage switch, whereas in the described generator, the formation of the output pulse can be triggered by both built-in control devices and a digital synchronization signal from an external control unit. In this case, the accuracy of locking the current-pulse start to the synchronization signal is a few nanoseconds. The controllability of the current generator based on the inductive storage allows one to use it in computer-aided systems for the experimental determination of pulse characteristics of GCs [2].

REFERENCES

1. Danilin, A.N., Kolobov, V.V., Selivanov, V.N., and Prokopchuk, P.I., *Sbornik dokladov devyatoi Rossiiskoi nauchno-tekhnicheskoi konferentsii po elektromagnitnoi sovmestimosti tekhnicheskikh sredstv i elektromagnitnoi bezopasnosti "EMS-2006"* (Proc. 9th Russ. Sci.-Techn. Conf. on Electromagnetic Compatibility of Technical Means and Electromagnetic Safety), St. Petersburg: VITU, 2006, p. 426.
2. Dzhura, D.A. and Selivanov, V.N., in *Trudy KNTs RAN. Energetika. Vyp. 7* (Proc. Kolsk. Sci. Center Russ. Acad. Sci. Energetics, no. 7), Apatity: Kol'sk. Nauchn. Tsentr Ross. Akad. Nauk, 2013, p. 73.
3. Danilin, A.N., Kuklin, D.V., and Selivanov, V.N., *Nauchno-Tekhnicheskie Vedomosti St. Petersb. Gos. Polutekh. Univ.*, 2010, no. 1, p. 250.

4. Bocharov, Yu.N., Korovkin, N.V., Krivosheev, S.I., and Shishigin, S.L., *Nauchno-Tekhnicheskie vedomosti St. Petersb. Gos. Polutekh. Univ.,* 2009, vol. 1, no. 89, p. 115.
5. Bessonov, L.A., *Teoreticheskie osnovy elektrotekhniki. Elektricheskie tsepi: Uchebnik* (Theoretical Foundations of Electrical Engineering. Electric Chains. A Handbook), Moscow: Gardariki, 2007.
6. Makashov, D., http://www.bludger.narod.ru/smps/Flyback-R01.pdf
7. Semenov, B.Yu., *Silovaya elektronika: ot prostogo k slozhnomu* (Power Electronics: From Simple to Complex), Moscow: Solon-Press, 2005.
8. About Magnetics: Leader in Powder Core, Ferrite Core, and Tape Wound Core Technology. http://www.mag-inc.com/company
9. Powder Cores with High a Saturation Induction. http://ferrite.ru/products/magnetics/powder-cores/
10. IRG7PH35UD Insulated gate bipolar transistor with ultra-low vf diode for induction heating and soft switching application. http://irf.ru/pdf/IRG7PH35UD1.pdf
11. ATmega48PA/88PA/168PA/328P Datasheet Summary. http://www.atmel.com/Images/8161s.pdf

Translated by N. Pakhomova